Available online at www.sciencedirect.com
SCIENCE DIRECT®
Thermochimica Acta 414 (2004) 59–63
thermochimica acta
www.elsevier.com/locate/tca

Study of oxidation properties and decomposition kinetics of three-dimensional (3-D) braided carbon fiber

Pengzhao Gao, Hongjie Wang*, Zhihao Jin

State Key Laboratory for Mechanical Behavior of Materials, School of Materials Science and Engineering, Xi'an Jiaotong University, Xi'an 710049, PR China

Received 21 May 2003; received in revised form 28 October 2003; accepted 14 November 2003

Abstract

The XRD, SEM, isothermal oxidation-weight loss and non-isothermal thermogravimetry (TG)–differential thermogravimetry (DTG) were used to study the oxidation properties and oxidation decomposition kinetics of three-dimensional (3-D) braided carbon fiber (abbreviated as fiber). The results showed that the non-isothermal oxidation process of fiber exhibited self-catalytic characteristic. The kinetic parameters and oxidation mechanism of fiber were studied through analyzing the TG and DTG data by differential and integral methods. The oxidation mechanism was random nucleation, the kinetic parameters were: $\lg A = 10.299\,\mathrm{min}^{-1}$; $E_a = 156.29\,\mathrm{kJ\,mol}^{-1}$.

Keywords: 3-D braided carbon fiber; Oxidation properties; Thermal analysis; Oxidation kinetics and mechanism

1. Introduction

Carbon fiber-reinforced composites (ceramic, glass, glass–ceramic and polymers, abbreviated as CFRCs) have received much attention in recent years. Their good mechanical, thermal and chemical properties, especially from the point of view of property/weight and property/cost ratios, make these materials widely applicable in many fields. Recently, attention has been focused on three-dimensional (3-D) braided carbon fiber-reinforced composites in order to meet mechanical and thermal properties requirements along the thickness of the composites [1].

However, carbon fiber exhibits a very poor oxidation resistance even at temperature as low as 700 K, although it has many advantages, such as low specific weight, and excellent mechanical strength at elevated temperatures. Consequently, the applications of CFRCs as high-temperature material have been mostly limited to inert atmosphere in order to prevent the oxidation degradation of carbon fiber [2,3]. Once the interfacial bond between fiber and matrix has been debonded by oxidation, a significant reduction in mechanical properties of the composite is unavoidable [4,5]. For example, flexural strength of carbon fiber-reinforced phenylethynyl-terminated poly(etherimide) composite decreased 50% when the oxygen partial pressure was 40.4 kPa and exposure time was 180 h [4]. Therefore, the oxidation behavior of fiber will affect the serve surrounding and life of CFRCs. Thermogravimetric analysis (TGA) is one of the quantitative analysis techniques to study the oxidation kinetics and mechanism of solid materials.

In the present work, the oxidation properties and decomposition kinetics of 3-D braided carbon fiber were studied by isothermal oxidation-weight loss by non-isothermal thermogravimetric (TG) and differential thermogravimetric (DTG) methods.

2. Experimental procedure

2.1. Experimental material

All of the 3-D braided carbon fiber used in this study was PAN-based carbon fiber (diameter about 10 μm) obtained from Lanzhou Carbon Plant, PR China.

2.2. Characterization of 3-D braided carbon fiber

The morphology of fiber was examined by the SEM (S-2700). The crystalline of fiber was examined by the XRD (Damax-2000).

* Corresponding author. Tel.: +86-29-2667942; fax: +86-29-2665443.
E-mail address: hjwang@mail.xjtu.edu.cn (H. Wang).

0040-6031/$ – see front matter © 2003 Elsevier B.V. All rights reserved.
doi:10.1016/j.tca.2003.11.017

2.3. The oxidation properties and decomposition kinetic experiments

A muffle furnace was used for the isothermal weight loss experiments, static air was employed and the temperature accuracy was estimated as ±10 K. The tests were carried out at temperature ranging from 573 to 973 K, interval 30 K, 15 min. The weight change was noted by electricity balance (with a sensitivity of ±0.1 mg).

The USA-TA5000 TG thermal analyzer was employed for the study of oxidation reaction kinetics and mechanism of fiber (thermobalance with a sensitivity of ±0.1 mg, at temperatures ranging from room temperature to 1273 K under static air, a rate of 10 K min^{-1}).

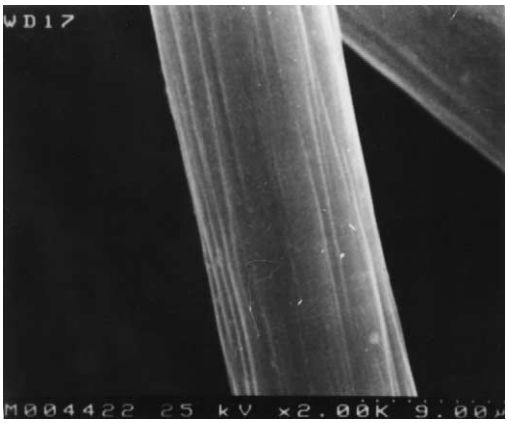

Fig. 1. The SEM photograph of fiber (2000×).

3. Results

3.1. Characterization of 3-D braided carbon fiber

The SEM photograph of fiber is shown in Fig. 1. The fiber surface was smooth and the striations along the fiber could be seen clearly. The XRD spectrum of fiber is shown in Fig. 2. It can be seen that the carbon fiber was graphite-like structure, which had the extended 2-D molecular chains [3].

3.2. Oxidation properties of 3-D braided carbon fiber

The isothermal oxidation-weight loss and Arrhenius curves of fiber are shown in Fig. 3. From the oxidation-weight loss curve (Fig. 3A), it is obvious that the fiber was oxidized from 723 K and it was burnt out at 923 K.

For the carbon materials, the oxidation-weight loss was proportional to the time when weight loss was below 70% [6] (Eq. (1)):

$$\frac{m_0 - m}{m_0} = kt \tag{1}$$

where m_0 is the initial quality of sample, m the quality of sample at time t, and k the reaction rate constant that was not changed at a fixed temperature.

The correlation of reaction rate constant with temperature followed the Arrhenius equation (Eq. (2)):

$$\ln k = \ln A - \frac{E_a}{R}\frac{1}{T} \tag{2}$$

where A is the pre-exponential factor, E_a the apparent activation energy of fiber oxidation in kJ mol^{-1}, T the abso-

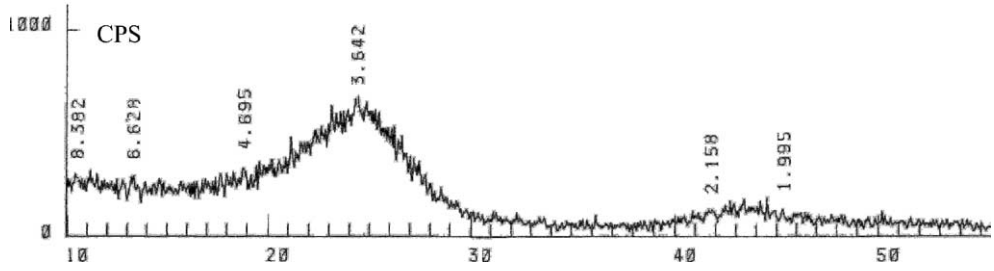

Fig. 2. The XRD spectrum of fiber.

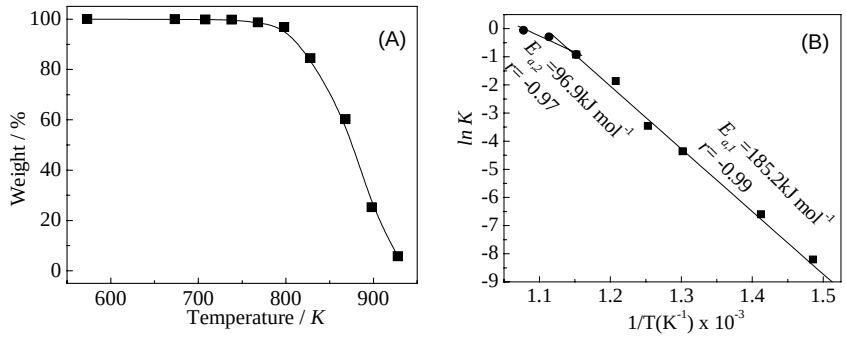

Fig. 3. The oxidation-weight loss (A) and Arrhenius (B) curves of fiber.

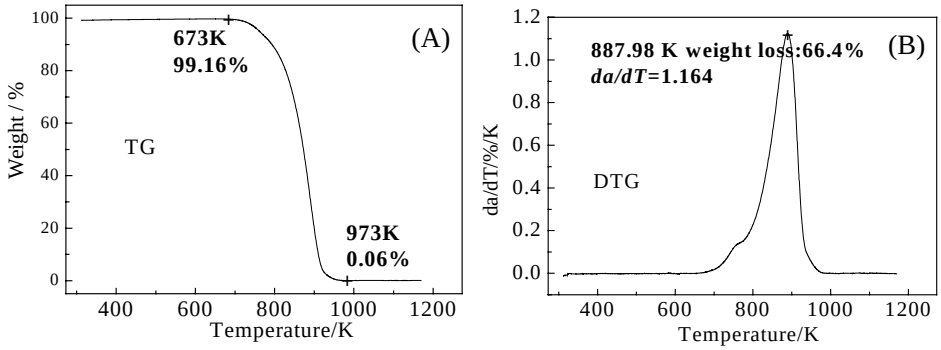

Fig. 4. TG (A) and DTG (B) curves of fiber.

lute temperature in K, and R the gas constant in J mol^{-1} K^{-1}.

Eq. (1) was changed and substituted into Eq. (2), and Eq. (3) was obtained:

$$\ln\left(\frac{m_0 - m}{m_0}\right) = \ln A + \ln t - \frac{E_a}{R}\frac{1}{T} \quad (3)$$

In the experimental conditions, the value of $(\ln A + \ln t)$ was constant. The Arrhenius curve could be obtained through plotting $\ln((m_0 - m)/m_0)$ versus $1/T$ (the data of m_0, m and T were obtained from Fig. 3A). The value of E_a could be obtained from the slope of this curve.

The Arrhenius curve of fiber is shown in Fig. 3B. It was easy to see that the curve consisted of two different slope lines, thus there were two different E_a values (185.2 and 96.9 kJ mol^{-1}), which were very close to the value obtained by Clark et al.'s work [7].

Two different E_a values meant that there were two different reaction mechanisms with the increase of temperature. This was an indication of a reaction mechanism transition in a temperature region around 873 K, as the result in Yin et al.'s work [2].

According to previous study [3], the oxidation mechanism of carbon materials could be divided into several steps, among which, the chemical reaction and the diffusion (mass transport) were two major limiting steps. The E_a, which represented the chemical reaction and gas diffusion, would be smaller than that obtained from a pure reaction controlled process, according to [2].

One may concluded that the oxidation of fiber at temperature ranges below 873 K was mainly controlled by chemical reaction, and at temperature ranges above 873 K, it was mainly controlled by chemical reaction and gas diffusion.

3.3. TG–DTG analysis of 3-D braided carbon fiber

The TG–DTG curves of fiber are shown in Fig. 4. From TG curve (Fig. 4A), it is obvious that the fiber was oxidized from 673 K and it was burnt out at 973 K. We can see that the result was consistent with that of Fig. 3A.

From DTG curve (Fig. 4B), it is obvious that the oxidation reaction rate (da/dT) of fiber was up to maximum when 66.31% fiber was burnt off. Thus, the characteristic of this reaction was self-catalytic, according to [3].

Initially, the active carbon atom (ACA) on fiber surface was small and the fiber had the lowest oxidation rate. As we knew that the extended 2-D chain structure of fiber should be broken off by the oxidation to form several smaller species, thereby increasing the ACA [3]. Thus, with the increasing of oxidation-weight loss, the amount of ACA increased, the reaction rate increased also. So the self-catalytic characteristic was displayed.

But there was a critical point, when the value of weight loss was bigger than 66.4%, the amount of species decreased

Table 1
Thermal decomposition data for 3-D braided carbon fiber from TG and DTG curves

T (K)	a	da/dT (% K^{-1})
783.01	0.082	0.173
788.02	0.090	0.189
793.23	0.100	0.206
798.16	0.110	0.224
803.20	0.122	0.249
808.16	0.134	0.273
813.23	0.149	0.304
818.18	0.164	0.335
822.97	0.181	0.376
827.98	0.200	0.418
832.99	0.222	0.468
838.00	0.246	0.521
843.00	0.273	0.578
847.96	0.303	0.633
852.92	0.336	0.697
858.10	0.373	0.765
863.17	0.414	0.848
868.12	0.456	0.920
873.12	0.504	0.999
878.03	0.555	1.069
883.03	0.610	1.123
887.98	0.666	1.164
892.98	0.724	1.156
898.14	0.782	1.096
903.13	0.835	1.012
908.08	0.882	0.871
913.07	0.920	0.675
918.03	0.948	0.454
923.08	0.96	0.253
928.06	0.973	0.157

with the increase of weight loss. And the oxidation rate decreased.

3.4. Kinetic study of 3-D braided carbon fiber

For the TG and DTG curves (Fig. 4), the equations of Achar–Brindley–Sharp–Wendworth [8,9], Satava–Sestak [10] and Coats–Redfern [11] were used to analysis the oxidation decomposition mechanism of fiber.

Achar–Brindley–Sharp–Wendworth equation:

$$\ln\left[\frac{1}{F(a)}\frac{\mathrm{d}a}{\mathrm{d}T}\right] = \ln\left(\frac{A}{\beta}\right) - \frac{E_\mathrm{a}}{R}\frac{1}{T} \tag{4}$$

Satava–Sestak equation:

$$\lg[G(a)] = \lg\left(\frac{AE_\mathrm{a}}{\beta R}\right) - 2.135 - \frac{0.4567E_\mathrm{a}}{R}\frac{1}{T} \tag{5}$$

Coats–Redfern equation:

$$\ln\frac{G(a)}{T^2} = \ln\left(\frac{AR}{\beta E_\mathrm{a}}\right) - \frac{E_\mathrm{a}}{R}\frac{1}{T} \tag{6}$$

where β is the heating rate, a the reaction fraction, and $F(a)$ and $G(a)$ the differential and integral mechanism functions, respectively.

The basic data of a, T and $\mathrm{d}a/\mathrm{d}T$ obtained by the TG–DTG curves are listed in Table 1. The integral ($G(a)$) and differential ($F(a)$) functions for the most common mechanism used in kinetic study of solid-state decomposition in this work are listed in Table 2 [12–14].

According to Eqs. (4)–(6), the values of E_a and A can be calculated from the slope and intercept of $\ln[(\mathrm{d}a/\mathrm{d}T)/F(a)]$, $\log[G(a)]$ and $\ln[G(a)/T^2]$ versus $1/T$ lines, respectively.

The values of $\ln[(\mathrm{d}a/\mathrm{d}T)/F(a)]$, $\log[G(a)]$, $\ln[G(a)/T^2]$ and $1/T$ for all possible mechanisms were calculated from the data of Tables 1 and 2.

The kinetic analyses were completed by the linear least-squares method on a computer. Kinetic parameters E_a, A, linear correlation coefficient (r) and standard deviation (S.D.) are listed in Table 3.

If the following conditions:

(1) the values of E_a were between 80 and 250 kJ mol^{-1} and the values of $\lg A$ were between 7 and 30 min^{-1}, which were obtained by the different methods were approximately equal;
(2) the linear relevant coefficient r was better (<-0.98);
(3) the standard deviation (S.D.) was small (<0.3);

were all satisfied at the same time. It can be concluded that the relevant function was the probable mechanism of oxidation thermal decomposition [15,16].

From the data in Table 3, it can be seen clearly that only function A1 satisfied the above-mentioned conditions. Thus, the possible mechanism was random nucleation. The kinetic parameters were $\lg A = 10.299\,\mathrm{min}^{-1}$, $E_\mathrm{a} = 156.29\,\mathrm{kJ\,mol}^{-1}$. We conclude that the kinetic equation for the thermal decomposition of fiber was: $\mathrm{d}a/\mathrm{d}T = (A/\beta)\exp(-E_\mathrm{a}/RT)(1-a)$.

4. Discussion

The oxidation mechanism of fiber was random nucleation; only one active nucleus on each species, which was as the result in Yang et al.'s work [17].

Table 2
Mechanism function of thermal decomposition kinetic equation [12–14]

Name of function	Type of mechanism		Form of function		Symbol
			$F(a)$	$G(a)$	
Avrami–Erofeev equation	Random nucleation	$n=1$	$1-a$	$-\ln(1-a)$	A1
		$n=2$	$2(1-a)[-\ln(1-a)]^{1/2}$	$[-\ln(1-a)]^{1/2}$	A2
		$n=3$	$3(1-a)[-\ln(1-a)]^{2/3}$	$[-\ln(1-a)]^{1/3}$	A3
Parabola law	1-D diffusion, decelerator a–t curve		$1/2a$	a^2	D1
Valensi equation	2-D diffusion, decelerator a–t curve		$[-\ln(1-a)]^{-1}$	$a+(1-a)\ln(1-a)$	D2
Jander equation	3-D diffusion, decelerator a–t curve		$1.5(1-a)^{2/3}[1-(1-a)^{1/3}]^{-1}$	$[1-(1-a)^{1/3}]^2$	D3
Anti-Jander equation	3-D diffusion		$1.5(1+a)^{2/3}[(1+a)^{1/3}-1]^{-1}$	$[(1+a)^{1/3}-1]^2$	D4
Ginstling–Brounstein equation	3-D diffusion, spherical symmetry		$1.5[(1-a)^{-1/3}-1]^{-1}$	$[1-2a/3]-(1-a)^{2/3}$	D5
Zhuralev–Lesokin–Tempelman equation	3-D diffusion		$1.5(1-a)^{4/3}[(1-a)^{-1/3}-1]^{-1}$	$[(1-a)^{-1/3}-1]^2$	D6
Chemical reaction equation	Phase boundary reaction	Cylindrical symmetry	$2(1-a)^{1/2}$	$1-(1-a)^{1/2}$	R2
		Spherical symmetry	$3(1-a)^{2/3}$	$1-(1-a)^{1/3}$	R3
	Reaction order	$n=2$	$(1-a)^2$	$(1-a)^{-1}$	F2

Table 3
Kinetic parameters of different method

No.	E_a (kJ mol^{-1})	lg A (min^{-1})	R	S.D.
Achar–Brindly–Sharp method				
A1	172.750	11.6711	−0.990	0.181
A2	93.227	6.658	−0.977	0.151
A3	66.719	4.912	−0.958	0.148
D1	163.601	10.538	−0.896	0.598
D2	210.890	13.298	−0.962	0.441
D3	272.896	16.642	−0.992	0.244
D4	134.559	7.654	−0.849	0.619
D5	232.594	14.04	−0.979	0.355
D6	393.802	24.438	−0.984	0.521
R2	112.297	7.472	−0.943	0.294
R3	132.448	8.595	−0.974	0.226
F2	293.656	19.469	−0.96123	0.623
Satava–Sestak method				
A1	151.244	11.298	−0.992	0.064
A2	75.622	6.888	−0.992	0.032
A3	50.415	5.493	−0.992	0.022
D1	212.549	14.453	−0.997	0.052
D2	235.586	15.682	−0.998	0.043
D3	267.115	17.119	−0.997	0.068
D4	193.170	12.187	−0.996	0.056
D5	245.822	15.707	−0.998	0.045
D6	343.765	22.207	−0.983	0.214
R2	125.788	9.348	−0.998	0.024
R3	133.558	9.675	−0.997	0.034
F2	114.974	9.791	−0.849	0.241
Coats–Redfern method				
A1	144.875	7.934	−0.991	0.147
A2	65.352	2.876	−0.989	0.072
A3	38.844	1.080	−0.987	0.047
D1	209.344	11.395	−0.997	0.122
D2	233.569	12.718	−0.9987	0.098
D3	266.725	14.266	−0.997	0.154
D4	188.965	9.044	−0.996	0.131
D5	244.333	12.78	−0.998	0.102
D6	347.329	19.58	−0.982	0.492
R2	118.106	5.814	−0.998	0.055
R3	126.277	6.196	−0.997	0.076
F2	106.735	6.174	−0.819	0.553

There was some reaction active point (RAP), which could react with oxygen, existed random and symmetrically in carbon fiber surface. When the carbon atom in RAP reacted with oxygen, one RAP would be consumed. But the extended 2-D chain structure of fiber should be broken off by the oxidation to form several smaller species. Every species has become a new RAP. Namely with the increased of oxidation, more and more new RAP were produced, the oxidation rate of fiber increased. The self-catalytic characteristic was observed.

As we knew, the amount of new produced RAP was determined by the length of 2-D molecular chain and fiber surface area, which all decreased with the increase of oxidation rate. But with the increase of oxidation rate, more and more RAPs were consumed.

Namely, with the increase of oxidation rate, the amount of new produced RAP decreased and more RAPs were consumed. Thus, when the amount of consumed was equal to that of produced RAP. The reaction rate was up to maximum (weight loss = 66.4%).

When the weight loss was bigger than 66.4%, the amount of consumed RAP by oxidation was bigger than that of new produced. The oxidation rate decreased with the increase of weight loss. In other words, the self-catalytic characteristic of fiber oxidation reaction could be explained through the oxidation decomposition mechanism.

5. Summary

1. The oxidation reaction of 3-D braided carbon fiber below 873 K was mainly controlled by chemical reaction and above 873 K was mainly controlled by chemical reaction and gas diffusion together.
2. The characteristic of the non-isothermal oxidation process was self-catalytic; the oxidation reaction rate was up to the maximum when 66.40% fiber was burnt off.
3. The oxidation mechanism was random nucleation; only one active nucleus on each species, the kinetic parameters were: $\lg A = 10.299\,\mathrm{min}^{-1}$; $E_a = 156.29\,\mathrm{kJ\,mol}^{-1}$. The kinetic equation was: $\mathrm{d}a/\mathrm{d}T = (A/\beta)\exp(-E_a/RT)(1-a)$.

Acknowledgements

This work was supported by the National Natural Science Foundation of China (No. 90305001).

References

[1] Y. Xu, L. Cheng, L. Zhong, et al., Mater. Sci. Eng. A 300 (2001) 196–202.
[2] Y. Yin, J.G. Binner, T.E. Cross, et al., J. Mater. Sci. 29 (1994) 2250–2254.
[3] L.R. Zhao, B.Z. Jang, J. Mater. Sci. 32 (1997) 2811–2819.
[4] T.A. Bullions, J.E. McGrath, A.C. Loos, Compos. Sci. Technol. 63 (2003) 1737–1748.
[5] S. Labruquére, J.S. Gueguen, R. Pailler, et al., J. Eur. Ceram. Soc. 22 (2002) 1023–1030.
[6] R. Luo, J. Cheng, T. Wang, Carbon 40 (2002) 1965–1972.
[7] D. Clark, N.J. Wadaworth, W. Watt, Carbon fibers. There place in modern technology, in: N.C.W. Judd, J. Mountfield, P.C. Oliver, D.M. Cohen (Eds.), Proceedings of the International Conference, Plastics Institute, London, February 1974, p. 44.
[8] B.N. Achar, G.W. Brindley, J.H. Sharp, in: Proceedings of the International Clay Conference, vol. 1, Jerusalem, 1996, p. 67.
[9] J.H. Sharp, S.A. Wendworth, Anal. Chem. 41 (14) (1969) 2060–2062.
[10] V. Satava, J. Sestak, J. Therm. Anal. 8 (3) (1975) 477–489.
[11] A.W. Coats, J.P. Redfern, Nature 201 (4914) (1964) 68–69.
[12] X. Gao, D. Dollimore, Thermochim. Acta 215 (1993) 47–55.
[13] M.A. Gabal, Thermochim. Acta 402 (2003) 199–208.
[14] R.M. Mahfouz, M.A.S. Monshi, N.M. Abd El-Salam, Thermochim. Acta 383 (2002) 95–101.
[15] T. Zhang, R. Hu, F. Li, Thermochim. Acta 244 (1994) 177–184.
[16] R. Hu, Z. Yang, Thermochim. Acta 123 (1988) 135–142.
[17] Y. Yang, F. He, M. Wang, et al., Tansu 1 (1998) 2–15.